Article

Volatile Selenium Flux from the Great Salt Lake, Utah

Ximena Diaz, William P. Johnson, Wade A. Oliver, and David L. Naftz

More About This Article

Additional resources and features associated with this article are available within the HTML version:

- Supporting Information
- Access to high resolution figures
- Links to articles and content related to this article
- Copyright permission to reproduce figures and/or text from this article

View the Full Text HTML

Volatile Selenium Flux from the Great Salt Lake, Utah

XIMENA DIAZ,[†,§]
WILLIAM P. JOHNSON,*,[†]
WADE A. OLIVER,[†] AND
DAVID L. NAFTZ[†,‡]

Department of Geology and Geophysics, University of Utah, 135 South 1460 East Salt Lake City, Utah 84112, and U.S. Geological Survey, 2329 West Orton Circle, Salt Lake City, Utah 84119

The removal mechanisms that govern Se concentrations in the Great Salt Lake are unknown despite this terminal lake being an avian habitat of hemispheric importance. However, the volatilization flux of Se from the Great Salt Lake has not been previously measured due to challenges of analysis in this hypersaline environment. This paper presents results from recent field studies examining the spatial distribution of dissolved volatile Se (areally and with depth) in the south arm (main body) of the Great Salt Lake. The analyses involved collection of dissolved volatile Se in a cryofocusing trap system via sparging with helium. The cryotrapped volatile Se was digested with nitric acid and analyzed by inductively coupled plasma mass spectrometry (ICP-MS). Results show concentrations of dissolved volatile Se that increase with depth in the shallow brine, suggesting that phytoplankton in the open waters and bioherms in shallow sites (<4 m in depth) may be responsible for volatile Se production. Volatile Se flux to the atmosphere was determined using mass transport models corrected to simulate the highly saline environment of the south arm of the Great Salt Lake. The estimated annual flux of volatile Se was 1455 kg/year within a range from 560 to 3780 kg Se/year for the 95% confidence interval and from 970 to 2180 kg Se/year within the 68% confidence interval.

Introduction

The Great Salt Lake (GSL), a shallow terminal hypersaline lake, was in the past considered a "dead" lake and a disposal system for waste effluents (*1*). As a meromictic lake, the south basin of the GSL has two layers, with a higher salinity (16−19%) higher density (1.16 g/mL) anoxic brine below 6.5−7 m depth, and a lower salinity (13−14%) lower density (1.10 g/mL) shallow brine above that depth. The maximum depth of the south arm of the GSL was 9 m, and the average surface area during the period of study was 1874.7 km². Sulfur-reducing bacteria have been identified in the underlying anoxic sediments and are likely responsible for observed mercury biomethylation in the anoxic water column (*2*). The deep anoxic waters of the lake were believed to immobilize

heavy metals, including Se, Hg, and As, as sulfide precipitates (*1*). However, recent studies indicate that precipitation as sulfides and removal via sedimentation may not be the dominant removal processes for trace metals, since wind-driven resuspension events and lake area decrease may reintroduce trace metals back into the water column, thereby reducing the net sedimentation removal of trace metals from the system (*3, 4*).

The GSL is a migratory bird habitat of hemispheric importance (*5*), and it feeds a 10−20 million pounds brine shrimp industry that is valued globally for high-protein brine shrimp cysts (*6*) which are purchased as food by the Asian tiger prawn industry.

Lately, the concern has been raised that Se levels in the GSL may become sufficient to yield toxic effects on avian wildlife (*7*), and this concern is heightened by the planned disposal of reverse osmosis rejected from groundwater treatment at the Jordan Valley Water Conservancy District (http://www.jvwcd.org/swjvgp/swjvgp.html). For this reason, a number of state, federal, and nongovernmental agencies are interested in better understanding of the cycling of trace metals in the GSL.

A previously uninvestigated (but possibly important) mechanism of permanent removal of Se from this shallow lake is volatilization. Se emissions to the atmosphere from natural sources have been estimated to be responsible for 50−70% of the total emission flux worldwide, with 60−80% of this flux coming from the oceans (*8, 9*). Studies performed in Europe showed that the amount of Se removed as volatile compounds from the Mediterranean Sea is 2.5 times higher than the total Se release to the atmosphere by fossil fuel combustion from the European countries (75 tons per year) (*8, 10*). Concentrations ranging from 0.45 to 3.54 pmol/L of volatile Se were reported from the Gironde Estuary (*8*). Volatile Se flux from the GSL has not been previously measured mainly due to challenges of analysis in this hypersaline environment.

Volatile Se species are produced by biomethylation of inorganic and organic Se species (*11*). The biotransformation of Se in a lake is mediated by diverse living organisms as fungi, microalgae, phytoplankton, zooplankton, and aerobic and anaerobic bacteria (*8, 11, 12*). A euryhaline bacteria (*Chlorella* species) isolated from hypersaline Se-contaminated evaporation ponds was shown to produce dimethyl selenide (*13*). Amouroux and Donard (*10*) found that dissolved volatile Se concentrations are directly proportional to algal biomass in open seawaters. Volatile Se species identified in the atmosphere are dimethyl selenide (DMSe), dimethyl diselenide (DMDSe), dimethyl selenone, and methane selenol, with DMSe being the most important in air as well as fresh and saline waters (*14*).

The south arm of the GSL presents appropriate characteristics to produce significant amount of volatile Se in its shallow and deep water. It has a distinctive photic zone in open waters varying from a measured minimum of 0.6 m in winter to a maximum of 3.1 m in fall. In the epilimnion, the productivity of phytoplankton is driven by dominant species like cyanobacteria *Nodularia spumigena*, diatom, and the green alga *Dunaliella viridis* (*15*). In shallow near-shore sediments, benthic organisms are prevalent such as brine fly larvae, periphyton, and cyanobacteria (*Aphanotece* sp.) which deposit stromatolites (*16, 17*). The objective of this work was to determine of the annual volatilization flux of Se using measured dissolved volatile Se concentrations and direct measurements of flux.

* Corresponding author phone: (801) 581-5033; fax: (801) 581-7065; e-mail: william.johnson@utah.edu.
† University of Utah.
‡ U.S. Geological Survey.
§ Current address: Department of Extractive Metallurgy, Escuela Politécnica Nacional, Quito, Ecuador.
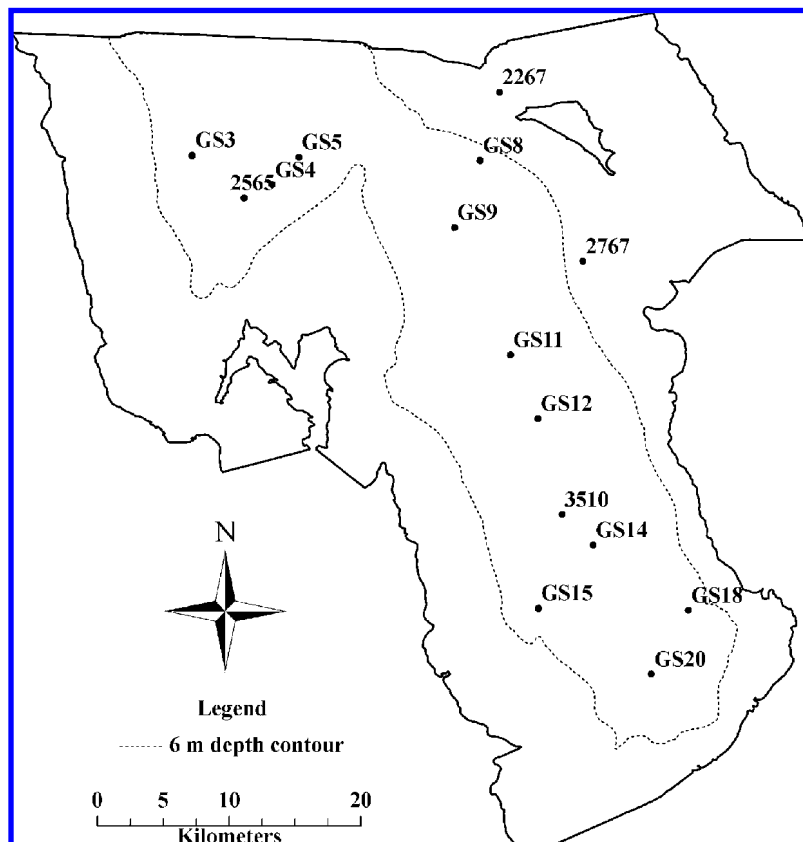
FIGURE 1. Volatile Se sampling locations, Great Salt Lake, UT. Contour shows the 6 m in depth boundary. Locations inside the boundary have depths between 6 and 9 m.

Materials and Methods

Location. The study location concerned the main body of the GSL, Utah. Monthly water samples were collected from September to December 2006 at 16 locations (14 sites with >6 m water column thickness, and two sites with <5 m water column thickness) at 1–3 depths per site in the south arm of the GSL to explore variations in volatile Se concentrations seasonally and spatially (areally and with depth). From May to August 2007, sampling was carried out at two deep sites (2265 and 3510) and one shallow site (2267). Water samples were collected at five depths in the deep sites and four depths in the shallow site in order to investigate the variation of dissolved volatile Se concentrations with depth. The purge and cryofocusing trap process to collect volatile samples was performed at the respective sampling sites on the lake in order to avoid degradation of the water samples during transport and holding. Direct measurements of volatilization of Se were taken at two primary locations (3510 and 2267) and one secondary location (2565) in the south arm of the GSL (Figure 1) in the summer of 2007.

Purge and Cryotrap System. Collection of volatile Se from the water involves a cryofocusing trap system following concepts used by researchers at the University of Pau in France (10). The system consists of a reactor (a modified desiccator) with a diffuser connected to a helium line. The reactor can sparge 7 L of hypersaline water. The cryotrap system purges the vast majority of volatile species present via continuous sparging with inert vapor. The vapor swept from the reactor moves via Teflon tubing to a glass water trap (−55 °C, dry ice/ethanol) to remove water from the flowing vapor. The vapor then enters a glass trap (−196 °C, liquid nitrogen) to trap the volatile compounds collected from the water. Studies demonstrate that the entire volume of water can be sparged at a helium flow rate of 500 mL/min for approximately 15 min. After collection, nitric acid is added
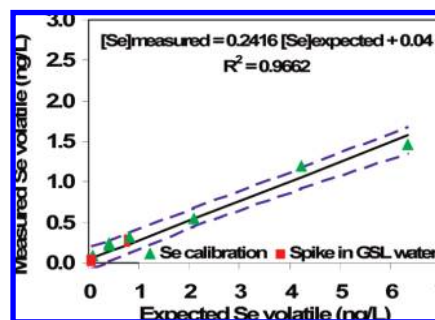

FIGURE 2. Calibration curve for dimethyl selenide using the purge and trap system.

to the glass trap to oxidize volatile Se compounds and convert them to their stable aqueous species. The closed trap is digested in a water bath at 75 °C for 3 h, and the solution is analyzed for Se by inductively coupled plasma mass spectrometry (ICP-MS) at the University of Utah Center for Water, Ecosystems, and Climate Science (CWECS) laboratory. The purge and cryofocusing trap system was calibrated with DMSe (Alfa Aesar, 99% purity) which is reported to be the most stable volatile Se compound in seawater and therefore the appropriate specie on which to base our study (11, 14, 18). This system was tested in the laboratory using GSL water spiked with pure DMSe. The analyzed spiked DMSe concentrations were equivalent to the expected value (within the 95% confidence limit) based on the calibration curve (Figure 2). Since measurements of distilled water yield apparent volatile Se concentrations of 0.04 ± 0.01 ng/L, the practical detection limit for volatile Se using the purge and trap system is 0.04 ng/L. These results demonstrate that the system can quantify volatile Se concentrations in the nanogram per liter range. The regressed recovery of dissolved volatile Se was 25% due to losses in the system; therefore,

measured values were corrected for 25% recovery according to the regression in Figure 2. Each time the system was calibrated, the average recovery rate was constant and highly reproducible (within the 95% CI, Figure 2). The losses yielding the 25% recovery likely include partitioning to stainless steel, ceramic, glass, and Teflon surfaces in the chamber and tubing and to epoxy sealant holding the lid of the chamber (which was a modified 9 L desiccator). Volatilization of DMSe out of the system is unlikely given that the system was sealed. Between samples, the entire system was thoroughly cleaned by rinsing five times with nitric acid (4 L, 2%) and distilled water (4 L). Tests demonstrated that dissolved volatile Se concentrations returned to background concentrations (0.04 ± 0.01 ng/L) after cleaning. The calibration curve was used to correct the values measured in the field. Laboratory tests were run using distilled water and GSL shallow brine water with and without spiking of DMSe to determine the analytical error. This error was determined to be 13%, which includes the error associated with the ICP-MS analyses. More information regarding ICP-MS analyses are provided in the Supporting Information.

Flux Calculation Models. To estimate the volatile Se flux from open water to the atmosphere, several models are available in the literature (19–22). These models have been used for estimating fluxes in fresh and seawater. The relationship between measured dissolved volatile Se concentrations, wind speed, and flux in these models is undoubtedly influenced by nonvolatilization processes such as biotransformation and photolysis, since these models were developed in real systems. We adopt these models under the assumption that the relationship between dissolved volatile Se concentrations, wind speed, and flux are similar in the GSL, with the modifications described below.

An expression for the volatile Se flux in the GSL is given below with the assumption that water to vapor mass transfer of DMSe in the GSL is kinetically controlled in the water phase, as opposed to the vapor phase (19).

$$\text{flux} = ak_w(C_{water}^{VSe} - C_{water}^{VSe,eq}) =$$
$$ak_w\left(C_{water}^{VSe} - \frac{C_{air}^{VSe}}{K_{H_{GSL}}'}\right) \quad (\text{mol/m}^2/\text{d})$$

where a is a unit correction factor (= 0.24), k_w is the water transfer velocity in the air−water interface (cm/h), C_{water}^{VSe} is the concentration of volatile Se in water (mol/m^3), $C_{water}^{VSe,eq}$ is the equilibrium concentration of volatile Se in water (mol/m^3), C_{air}^{VSe} is the concentration of volatile Se in air (mol/m^3), and $K_{H_{GSL}}'$ is the dimensionless Henry's constant for volatile Se for the GSL.

Dimensionless Henry's Constant Correction. The dimensionless Henry's constant ($K_{H_{GSL}}'$) and the water mass transfer velocity in the air−water interface (k_w) were determined using empirical models from the literature (19–22). These models are based on wind velocity, water temperature, viscosity, and diffusivity of the volatile species. The viscosity, diffusivity, and dimensionless Henry's constant each require corrections for the salinity of the GSL, which is 3−5 times saltier than the ocean.

An equation to estimate the dimensionless Henry's constant for DMSe as a function of temperature was developed by Guo et al. (23), whereas a salinity correction was provided by Schwarzenbach et al. (19), yielding

$$K_{H_{GSL}} = 0.0248 \exp(0.0418T) \times 10^{K^s[\text{salt}]_{\text{tot}}}$$

where K^s is the salinity constant and $[\text{salt}]_{\text{tot}}$ is the total molar concentration of salt. The K^s for DMSe was not available from the literature, whereas a value for dimethyl sulfide (DMS) was available and equal to 0.17 L/mol from Schwarzenbach

et al. (19) and was used on the basis of its similarity to DMSe (8).

For minimum and maximum surface temperatures measured on the lake (2 °C in winter and 30 °C in summer) and a mean salt concentration of 2.45 M (based on major salts presents in the shallow brine: NaCl, MgCl$_2$, MgSO$_4$, K$_2$SO$_4$, and CaSO$_4$), values of the $K_{H_{GSL}}'$ ranged from 0.070 to 0.227, indicating the DMSe volatilization is water-phase-controlled under these conditions (19).

Water Transfer Velocity Using the Estuarine Model. The water transfer velocity (k_w) was calculated using a relationship with wind velocity developed in the Hudson Estuary by Clark et al. (20), which was developed for a Schmidt number (Sc) equal to 600. According to the boundary layer model (19), the Sc was corrected for two wind velocity regimes. This so-called estuarine model is as follows:

$$k_w(\text{cm/h}) = \left(\frac{Sc}{600}\right)^{-1/2}(2 + 0.24u_{10}^2) \quad \text{for} \quad u_{10} > 5 \text{ m/s}$$

$$k_w(\text{cm/h}) = \left(\frac{Sc}{600}\right)^{-2/3}(2 + 0.24u_{10}^2) \quad \text{for} \quad u_{10} \le 5 \text{ m/s}$$

where Sc is the Schmidt number and u_{10} is the wind velocity measured 10 m over the surface of the lake. Saltzman and King (24) defined a Schmidt number for DMS as a function of temperature (in °C) and corrected for the seawater salinity (via coefficients) as follows:

$$Sc_{DMS}^{\text{seawater}} = 2674.0 - 147.12T + 3.726T^2 - 0.038T^3$$

Water Transfer Velocity Using the Modified Liss and Merlivat Model. An alternative approach is provided by the modified Liss and Merlivat model (19, 21, 22), the results of which corroborate the estuarine model. This model, which was also corrected for the Schmidt number according to the boundary layer model (19), defined three wind velocity regimes:

$$k_w(\text{cm/h}) = \left(\frac{Sc}{600}\right)^{-2/3}(2.34) \quad \text{for} \quad u_{10} < 4.2 \text{ m/s}$$

$$k_w(\text{cm/h}) = \left(\frac{Sc}{600}\right)^{-1/2}(2.85u_{10} - 9.65)$$
$$\text{for} \quad 4.2 \text{ m/s} < u_{10} < 13 \text{ m/s}$$

$$k_w(\text{cm/h}) = \left(\frac{Sc}{600}\right)^{-1/2}(5.9u_{10} - 49.3) \quad \text{for} \quad u_{10} > 13.6 \text{ m/s}$$

Diffusive Flux. The diffusive flux can be calculated assuming that diffusion is the limiting mass transfer process in water, as follows:

$$J = D_e \frac{\Delta C}{\Delta x}$$

where J is the diffusive flux (g/cm^2/year), D_e is the effective diffusion coefficient (cm/s), ΔC is the concentration gradient (ng/L), and Δx is the difference in depth (m). The diffusion coefficient for DMSe can be calculated using the diffusion coefficient for DMS as function of temperature, corrected for seawater, according to Saltzman and King (24):

$$D_{DMSe} \approx D_{DMS} = 0.0192 \exp(-18.1/RT)$$

where D_{DMSe} is the diffusion coefficient for DMSe (cm/s), R is the gas constant (kJ/mol K), and T is the temperature (K).

Wind Velocity and Atmospheric Temperature. Wind velocity and atmospheric temperature data from January 2006 to August 2007 were obtained from the MesoWest station at Hat Island. Weekly surface water temperatures were obtained using AVHRR (advanced very high resolution radiometer). The AVHRR is a scanner mounted on National Oceanic and Atmospheric Administration (NOAA) polar-orbiting satellites for measuring visible and infrared radiation
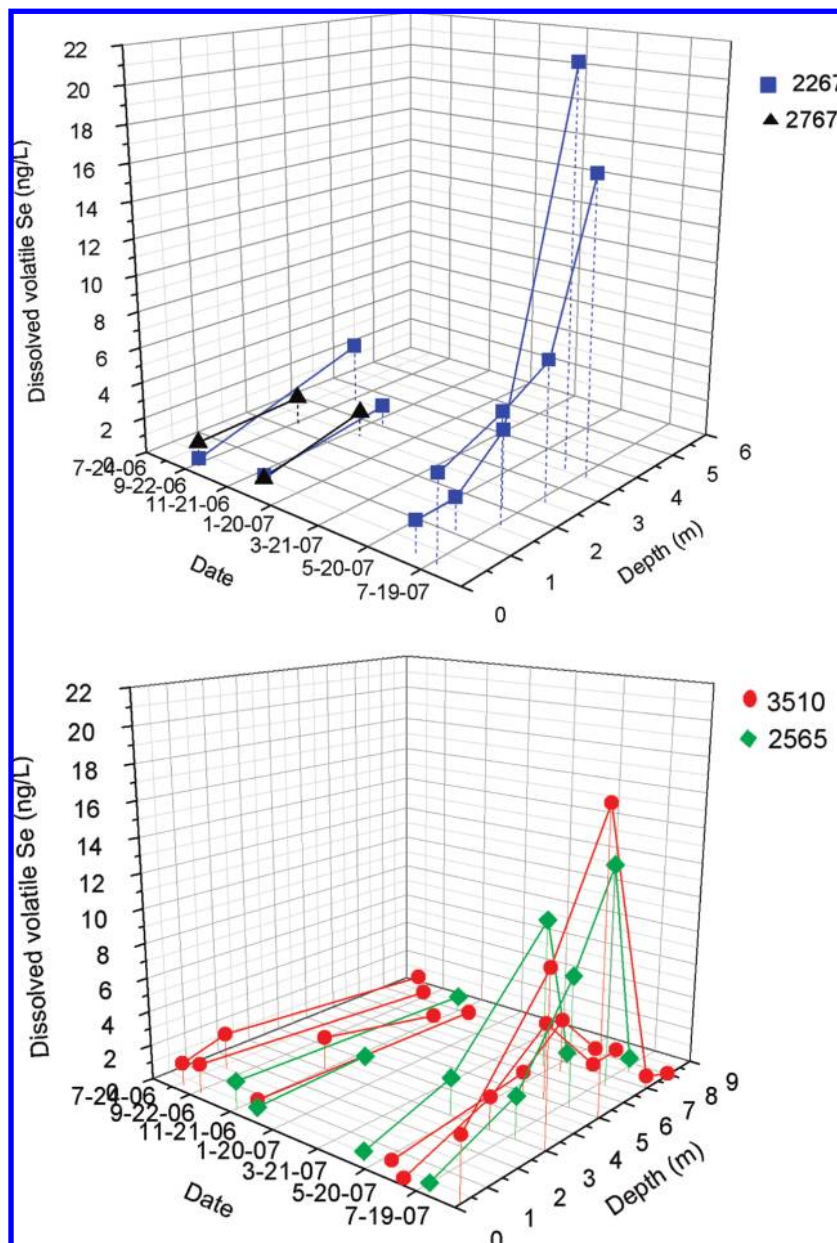
FIGURE 3. Dissolved volatile Se concentration results. Top: for shallow sites 2267 and 2767. Bottom: for deep sites 2565 and 3510 (shallow and deep brine layers). For any given site, the data shows same-day measurements at different depths. Data from July 2006 to August 2007.

reflected from vegetation, cloud cover, shorelines, water, snow, and ice. (ESRI Support Center, http://support.esri.com/index.cfm?fa=homepage.homepage). The data were obtained for the period January 2006 to December 2006, from the Department of Meteorology at the University of Utah. Comparisons were made between the AVHRR data (January 2006 to December 2006) and thermistor measurements in Gunnison Bay (January 2006 to August 2007) to ensure that the AVHRR data correctly represented water surface temperature during the period of study (Figure S1 in the Supporting Information). The estimated error for wind velocity measurement is 2.5 m/s (*25*). The estimated error for temperature measurement from an AVHRR is 0.5−1 °C (*26*).

Lake Elevation and Lake Surface Area. Lake elevation data were obtained from the USGS gage at the Saltair boat harbor. Surface area of the lake, used to calculate the cumulative volatile Se flux from the lake, was corrected for lake elevation according the data summarized by Baskin (*27*). Water surface elevations reported at the USGS GSL gages are considered to be accurate within ±0.10 ft of the datum in use (http://ut.water.usgs.gov/gsl%20corr/gslcorrection.htm).

Propagation of Error. The propagation of error in the calculation of the volatile Se flux was based on the estimated errors of the individual parameters used (wind velocity, surface water temperature, lake area, and dissolved volatile Se concentration). Detailed calculation methodology and results are presented in the Supporting Information.

Direct Measurements. An emission isolation flux chamber (St. Croix Sensory, Inc.) was used to collect volatilized Se from the surface of the lake. Helium gas was swept through the chamber to drive volatile gases coming from the lake into a cryotrap (liquid nitrogen) held at −170 °C by a Watlow PID temperature controller connected to a temperature sensor (PT-103 a.m. platinum RTD, Lakeshore Cryotronics, Inc.) and a cartridge heater (3039-002, Cryogenic Control Systems, Inc.). Volatile Se was oxidized with HNO_3 and analyzed via ICP-MS. More details are presented in the Supporting Information.
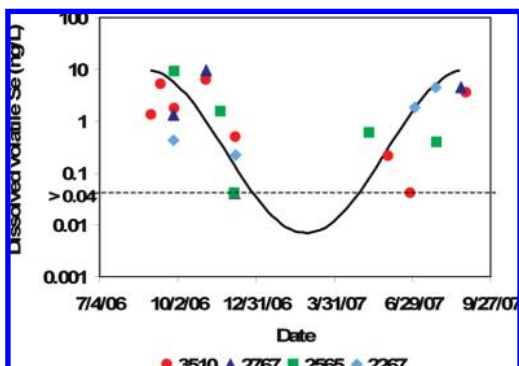
FIGURE 4. Concentration of dissolved volatile Se collected at 0.2−0.5 m from September 2006 to August 2007. The trendline shows sinusoidal fit to the data. The lower quantification limit of 0.04 ng/L is shown as a dashed horizontal line.

Results

Volatile Selenium Concentrations. Concentrations of dissolved volatile Se showed no apparent spatial trend in the main body of the lake (Figure S2 in the Supporting Information). Dissolved volatile Se concentrations increased with depth in the shallow brine layer (Figure 3), for the majority of sampling periods and sites where multiple depths were measured during the same day in the shallow brine layer. Dissolved volatile Se concentrations for depths below 6.0 m decreased with depth, for all sampling periods and sites where multiple depths were measured on the same day (Figure 3).

The average volatile Se concentrations in water were reduced during the winter and elevated during spring, summer, and fall (Figure S3 in the Supporting Information), coincident with warmer temperatures and increased net primary productivity. During the course of the investigation, average concentrations (across the entire lake and entire water column) of dissolved volatile Se ranged from 2.4 ng/L (within a range from 0.1 to 9.2 ng/L) in September 2006 to 0.31 ng/L (within a range from 0.04 to 1.2 ng/L) in early December 2006 and 6.9 ng/L in July 2007 (within a range from 0.1 to 22.7 ng/L). This temporal trend is also reflected
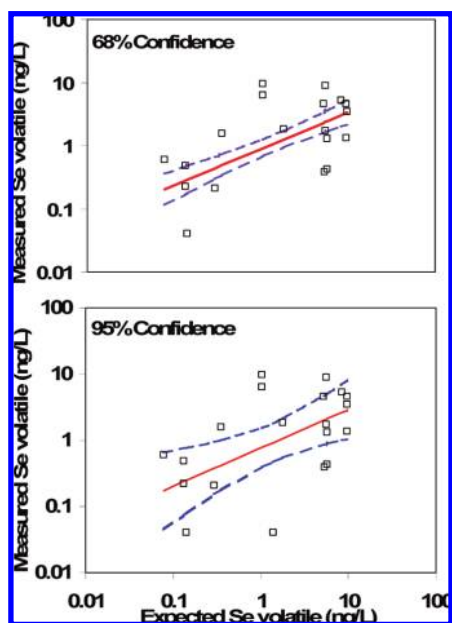

FIGURE 5. Determination of the confidence interval (CI) using expected vs measured data of near-surface volatile Se concentrations. Expected values corresponded to data obtained from the sinusoidal function (Figure 4). Top: 68% CI. Bottom: 95% CI.
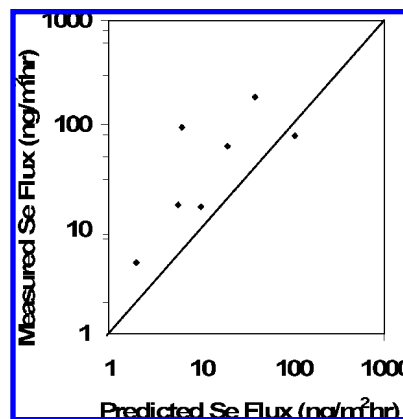

FIGURE 6. Correlation between the corrected measured volatile Se flux and the predicted volatile Se flux. Direct flux was measured using a flux chamber (details in the Supporting Information). Predicted data was obtained from the estuarine volatilization flux model. Dissolved volatile Se samples were collected at the same time and location as the direct flux measurements.

in the multiple-depth plots shown in Figure 3 for the shallow and deep brines.

The average dissolved volatile Se concentration from September 2006 to August 2007 was 3.0 ng/L (within a range from 0.04 to 22.7 ng/L). This value represents 0.6% of the average total Se concentration in the water column (500 ng/L, mainly as selenate (28)). Although this fraction seems negligible, its significance of course depends on the residence time of dissolved volatile Se in the lake. The vast surface area of the GSL relative to its depth (Figure S4 in the Supporting Information) may support significant mass transfer across the atmosphere−water interface.

Volatile Selenium Flux. Flux estimates were based on dissolved volatile Se concentrations at depths of 0.2−0.5 m from the surface, near the interface, where volatilization occurs. These near-surface concentrations indicate decreased of dissolved volatile Se concentration during winter and so were fitted using a sinusoidal function shown in Figure 4, according to the following equation:

$$C_{\text{water}}^{\text{VSe}} = 10^{\{A+B\sin[(t-C)\pi/D]\}}$$

where A, B, C, and D are constants and where the near-surface dissolved volatile Se concentration is ng Se/L.

The constants A through D were adjusted to yield the geometric mean (0.999 ng/L) and the geometric standard deviation (5.9) of the data. Measurements were not taken between December 15, 2006 and April 15, 2007, due to logistical reasons. The corresponding values of the constants are shown in the equation below.

$$C_{\text{water}}^{\text{VSe}} = 10^{\{-0.5815+1.5741\sin[(t-30)\pi/185]\}}$$

Estimation of the Annual Volatile Se Flow. The annual Se flow was estimated by integration of calculated volatile Se fluxes using recorded wind, temperature data, and lake surface area. The volatile Se flow estimates were integrated from the estuarine and the modified Liss and Merlivat fluxes over time using measured wind velocities (10 m above lake surface), water temperatures (at lake surface), and lake surface area variations for the 1 year period of study as described in the Materials and Methods. The integration assumed an instantaneous response of volatile Se flux to changes in wind velocity and water temperature (the measured parameter values are shown for the period of study in Figure S5 in the Supporting Information).

During integration, the following data frequencies were used for the lake area, temperature, and wind data: daily

TABLE 1. Comparison Results with Studies in the Mediterranean Sea[a]

source	mean concentrations of dissolved Se (nmol Se/L)	mean concentrations of dissolved volatile Se (pmol Se/L)	mean volatile Se flux (nmol/m² year)	mean volatile Se flow (kg Se/year)	area (km²)
east Mediterranean (7, 34)	0.5–0.9	0.35	442	105 000	2.511×10^8
Gironde Estuary (7)	1.0	2.48	810–3240	64–256	1000
Great Salt Lake, UT	6.3	9.17[b]	8250	1455	1874.7

[a] The mean flux was calculated using the modified Liss and Merlivat model for the south arm of the GSL. [b] Geometric mean.

average for lake area, weekly average for water temperature, and 1.5 h intervals for wind speed. The cumulative integrated flow is shown as a function of time in the Supporting Information (Figure S6). Integration of the volatile Se flow yielded an annual loss to the atmosphere of 2108 kg using the estuarine model and 1455 kg using the modified Liss and Merlivat approach.

The uncertainty range for the volatile Se flow was estimated using confidence intervals (CIs). The 95% (2σ) and the 68% (1σ) CIs for the near-surface dissolved volatile Se concentration were determined using the logarithms of the dissolved volatile Se concentration data obtained from the sinusoidal function (expected data) and the measured data (Figure 5). The antilog transformed arithmetic mean (of the log transformed data) yielded the geometric mean of the arithmetic data. The ratios of the arithmetic (antilog transformed) CI to the geometric mean yielded the geometric standard deviation around this mean. Values of 2σ (geometric) ranged from 2.0 to 3.8 (2.6 average) for the 95% CI, and values of σ (geometric) ranged from 1.4 to 1.8 (1.5 average) for the 68% CI (Figure 5).

The resulting estimated volatile Se flows using the estuarine model range (around the mean of 2108 kg Se/year) from 820 to 5450 kg Se/year within the 95% CI and from 1380 to 3210 kg Se/year within the 68% CI. With the use of the modified Liss and Merlivat model, the range (around the mean of 1455 kg Se/year) was 560–3780 kg Se/year within the 95% CI and from 970 to 2180 kg Se/year within the 68% CI.

Direct measurements of volatile Se flux were conducted using a flux chamber. Near-surface volatile Se samples in the water were collected simultaneously to correlate the measured data with the predicted volatile Se flux. Corrected measured Se fluxes (explained below) were generally higher (e.g., a factor of 2) than the predicted volatile Se flux estimated using the estuarine model (Figure 6). The need for correction of directly measured fluxes was indicated by calibration tests under highly controlled conditions, which showed that 10% of actual flux was captured by direct measurement (likely due to partitioning to surfaces). The similarity of corrected directly measured fluxes and estimated fluxes verified the ability of the models to provide reasonable estimates of volatile Se flux. Details regarding the direct measurements of volatile Se flux are provided in the Supporting Information.

Discussion

The observed increase in dissolved volatile Se concentrations with depth would implicate the underlying sediment as the source if it were not for the dramatic decrease in dissolved volatile Se concentrations in the deep brine layer relative to the shallow brine layer (Figure 3). Hence, the observed trends indicate a source within the shallow brine layer, quite possibly phytoplankton, as observed in the Mediterranean Sea (10). Other possible sources include bioherms (stromatolites) that occur where the lake bottom is shallow (and the anoxic deep brine layer is absent). Given a source within the shallow brine layer, steady-state diffusion of dissolved volatile Se to the surface would yield linear gradients in Se concentration as a function of depth. The concave (toward the surface) Se concentration gradients (Figure 3) cannot be produced by steady-state diffusion and indicate depletion of Se from the shallow brine via convection (lake mixing) (e.g., ref 29), bacterial consumption, or photolysis similar of what was observed to DMS in the North Sea (30). A diffusive flux of dissolved volatile Se based on a linear approximation of the observed gradient in the shallow brine (Figure 3) yields a flow of 7.3×10^{-2} kg Se/year. This extremely small flow would represent the quiescent lake, which based on the concave (toward surface) Se concentration gradients and the well-observed frequent wind mixing of the lake (4), we believe is far smaller than the actual flux.

The lower estimated annual volatile Se flux from the modified Liss and Merlivat model relative to the estuarine model results from the latter taking into account the turbulence created from the water friction over the lake bottom (appropriate for rivers, estuaries, and shallow lakes), which increases the water mass transfer velocity (20, 31). The modified Liss and Merlivat model is widely used and was used here in order to compare our results with results from the Mediterranean Sea (8).

The dissolved volatile Se concentrations in the GSL are between 4 and 30 times higher than those obtained in similar studies carried out in the Mediterranean Sea (Table 1). The total dissolved Se concentration in the GSL was 6–12 times higher than in the Mediterranean Sea (Table 1). The estimated volatile Se fluxes from the GSL showed also higher values (between 2.5 and 20 times higher) than those in the Mediterranean Sea (Table 1). The higher volatile Se fluxes in the GSL are supported by the higher dissolved volatile Se concentrations, which themselves may be related to high concentrations of phytoplankton and zooplankton in the lake, as indicated by chlorophyll *a* concentrations near the lake surface, which were 1–2 orders of magnitude higher than the values observed in the Mediterranean Sea (Table S2 in the Supporting Information; and ref 10). Amouroux and Donard (10) found a linear correlation between dissolved volatile Se concentrations and chlorophyll *a* in the open waters of the Mediterranean Sea, but not in the bay waters. The difference was suggested to be due to different types of phytoplankton populations in those areas (10). Archer et al. (32) studying the DMS production in the North Sea also attributed to the phytoplankton taxonomic differences the production rate of DMS in sea waters. Our results did not show correlation between the dissolved volatile Se and the phytoplankton concentrations (Figure S6 in the Supporting Information), and this may be due to different populations of volatile Se generators in the lake. More studies would be needed to clarify the cause of the particular sources of dissolved volatile Se. A comparison of the annual Se loss via volatilization and sedimentation to Se input via inflow is provided in Diaz et al. (33).

Supporting Information Available

Additional figures and tables supporting this work, as well as an explanation of error propagation for the predicted flux estimations and details regarding direct measurements of Se flux. This material is available free of charge via the Internet at http://pubs.acs.org.

Literature Cited

(1) Tayler, P. I.; Hutchinson, L. A.; Muir, M. K. Heavy metals in the Great Salt Lake, Utah. In *Great Salt Lake a Scientific, Historical and Economic Overview*; Gwynn, J. W., Ed.; Utah Geological and Minerals Survey: Salt Lake City, UT, 1980; Bulletin 16, pp 195−199.

(2) Naftz, D.; Angeroth, C.; Kenney, T.; Waddell, B.; Darnall, N.; Silva, S.; Perschon, C.; Whitehead, J. Anthropogenic influences on the input and biogeochemical cycling of nutrients and mercury in Great Salt Lake, Utah, USA. *Appl. Geochem.* **2008**, *23* (6), 1731–1744.

(3) Oliver, W. A. Selenium removal processes from Great Salt Lake, Utah: Estimating sedimentation and verifying volatilization fluxes. M.Sc. Thesis, University of Utah, Salt Lake City, UT, 2008.

(4) Beisner, K. R. Selenium and trace element mobility affected by periodic interruption of meromixis in the Great Salt Lake, Utah. M.Sc. Thesis, University of Utah, Salt Lake City, UT, 2008.

(5) Aldrich, T. W.; Paul, D. S. Avian ecology of Great Salt Lake. In *Great Salt Lake: An Overview of Change*; Gwynn, J. W., Ed.; Utah Department of Natural Resources Special Publication: Salt Lake City, UT, 2002; pp 343−374.

(6) Isaacson, A. E.; Hachman, F. C.; Robson, R. T. The economics of Great Salt Lake. In *Great Salt Lake: An Overview of Change*; Gwynn, J. W., Ed.; Utah Department of Natural Resources Special Publication: Salt Lake City, UT, 2002; pp 187−200.

(7) Johnson, W. P.; Conover, M.; Wurtsbaugh, W.; Adams, J. Conceptual model for selenium cycling in the Great Salt Lake, Utah; DEQ—Division of Water Quality: Salt Lake City, UT, 2006; available at www.deq.utah.gov/Issues/GSL_WQSC/docs/051408_Appendix_A.pdf.

(8) Amouroux, D. Etude du cycle biogeochimique du selenium a l'interface ocean−atmosphere. Ph.D. Thesis, University of Bordeaux I, Talence, France, 1995.

(9) Mosher, B. W.; Duce, R. A.; Prospero, J. M.; Savoie, D. L. Atmospheric selenium geographical distribution and ocean to atmosphere flux in the Pacific. *J. Geophys. Res.* **1987**, *92* (D11), 13277–13287.

(10) Amouroux, D.; Donard, O. F. X. Maritime emission of selenium to the atmosphere in eastern Mediterranean seas. *Geophys. Res. Lett.* **1996**, *23* (14), 1777–1780.

(11) Neumann, P. M.; De Souza, M. P.; Pickering, I. J.; Terry, N. Rapid microalgal metabolism of selenate to volatile dimethylselenide. *Plant Cell Environ.* **2003**, *26*, 897–905.

(12) Karlson, U.; Frankenberger, W. T., Jr.; Spencer, W. F. Physicochemical properties of dimethyl selenide and dimethyl diselenide. *J. Chem. Eng. Data* **1994**, *39*, 608–610.

(13) Fan, T. W.-M.; Lane, A. N.; Higashi, R. M. Selenium biotransformations by a euryhaline microalga isolated from a saline evaporation pond. *Environ. Sci. Technol.* **1997**, *31*, 569–576.

(14) Tessier, E.; Amouroux, D.; Donard, O. F. X. Biogenic volatilization of trace elements from European estuaries. In *Biogeochemistry of Environmentally Important Trace Elements*; Cai, Y., Braids, O. C., Eds.; American Chemical Society: Washington, DC, 2003; Chapter 12, pp 151−165.

(15) Marcarelli, A. M.; Wurtsbaugh, W. A.; Griset, O. Salinity controls phytoplankton response to nutrient in the Great Salt Lake, Utah, USA. *Can. J. Fish. Aquat. Sci.* **2006**, *63*, 2236–2248.

(16) Wurstbaugh, W. A. Food-web modification by an invertebrate predator in the Great Salt Lake (USA). *Oecologia* **1992**, *89*, 168–175.

(17) Pedone, V. A.; Folk, R. L. Formation of aragonite cement by nannobacteria in the Great Salt Lake, Utah. *Geology* **1996**, *24* (8), 763–765.

(18) Amouroux, D.; Tessier, E.; Donard, O. F. X. Volatilization of organotin compounds from estuarine and coastal environments. *Environ. Sci. Technol.* **2000**, *34*, 988–995.

(19) Schwarzenbach, R. P.; Gschwend, P. M.; Imboden, D. M. *Environmental Organic Chemistry*, 2nd ed.; Wiley-Interscience: Hoboken, NJ, 2003.

(20) Clark, J. F.; Schlosser, P.; Simpson, H. J.; Stute, M.; Wanninkhof, R.; Ho, D. T. Relationship between gas transfer velocities and wind speeds in the tidal Hudson River determined by the dual tracer technique. In *Air−Water Gas Transfer*; Jähne, B., Monahan, E. C., Eds.; AEON Verlag: Hanau, Germany, 1995; pp 785−800.

(21) Livingstone, D. M.; Imboden, D. M. The non-linear influence of wind-speed variability on gas transfer in lakes. *Tellus* **1993**, *45B*, 275–295.

(22) Liss, P. S.; Merlivat, L. Air−sea gas exchange rates: Introduction and synthesis. In *The Role of Air−Sea Exchanges in Geochemical Cycling*; Buat-Ménard, P., Ed.; D. Reidel Publishing Company: Dordrecht, The Netherlands, 1986; pp 113−127.

(23) Guo, L.; Jury, W. A.; Frankenberger, W. T., Jr. Measurement of the Henry's constant of dimethyl selenide as a function of temperature. *J. Environ. Qual.* **2000**, *29* (5), 1715–1717.

(24) Saltzman, E. S.; King, D. B. Experimental determination of the discussion coefficient of dimethyl sulfide in water. *J. Geophys. Res.* **1993**, *98* (C9), 16481–16486.

(25) Horel, J. University of Utah, Salt Lake City, UT. Personal communication, 2007.

(26) Crosman, E.; Horel, J. Remote sensing of the temperature of the Great Salt Lake. *J. Geophys. Res. C*, submitted for publication, **2006** available at http://www.met.utah.edu/research/saltlake/presentations/jgr-oceans-paper.

(27) Baskin, R. L. Calculation of area and volume for the south part of the Great Salt Lake, Utah; Open-File Report 2005-1327; U.S. Department of Interior, U.S. Geological Survey: Reston, VA, 2005.

(28) Brix, K. V.; DeForest, D. K.; Cardwell, R. D.; Adams, W. J. Derivation of a chronic site-specific water quality standard for selenium in the Great Salt Lake, Utah, USA. *Environ. Toxicol. Chem.* **2004**, *23*, 606–612.

(29) Bird, R. B.; Stewart, W. E.; Lightfoot, E. N. *Transport Phenomena*; John Wiley and Sons: New York, 2002.

(30) Archer, S. D.; Gilbert, F. J.; Nightingale, P. D.; Zubkov, M. V.; Taylor, A. H.; Smith, G. C.; Burkill, P. H. Transformation of dimethylsulphoniopropionate to dimethyl sulphide during summer in the North Sea with an examination of key processes via a modeling approach. *Deep-Sea Res., Part II* **2002**, *49*, 3067–3101.

(31) Raymond, P. A.; Cole, J. J. Gas exchange in rivers and estuaries: Choosing a gas transfer velocity. *Estuaries* **2001**, *24*, 269–274.

(32) Archer, S. D.; Smith, G. C.; Nightingale, P. D.; Widdicombe, C. E.; Tarran, G. A.; Rees, A. P.; Burkill, P. H. Dynamics of particulate dimethylsulphoniopropionate during a Lagrangian experiment in the northern North Sea. *Deep-Sea Res., Part II* **2002**, *49*, 2979–2999.

(33) Diaz, X.; Johnson, W. P.; Naftz, D. L. Selenium mass balance in the Great Salt Lake, Utah. *Sci. Total Environ.*, in press.

(34) Conde, J. E.; Sanz Alaejos, M. Selenium concentrations in natural and environmental waters. *Chem. Rev.* **1997**, *97* (6), 1979–2004.

ES801638W